JACS
JOURNAL OF THE AMERICAN CHEMICAL SOCIETY

COMMUNICATION

pubs.acs.org/JACS

# Noble-Metal-Free Bimetallic Nanoparticle-Catalyzed Selective Hydrogen Generation from Hydrous Hydrazine for Chemical Hydrogen Storage

Sanjay Kumar Singh,[†,‡] Ashish Kumar Singh,[‡] Kengo Aranishi, and Qiang Xu*

National Institute of Advanced Industrial Science and Technology (AIST), Ikeda, Osaka 563-8577, Japan

Supporting Information

**ABSTRACT:** Noble-metal-free nickel−iron alloy nanoparticles exhibit excellent catalytic performance for the complete decomposition of hydrous hydrazine, for which the NiFe nanocatalyst, with equimolar compositions of Ni and Fe, shows 100% hydrogen selectivity in basic solution (0.5 M NaOH) at 343 K. The development of low-cost and high-performance catalysts may encourage the effective application of hydrous hydrazine as a promising hydrogen storage material.

Nanosized bimetallic heterogeneous catalysts, especially those based on nonprecious, low-cost, and abundant metals, are highly demanded for various interdisciplinary chemical processes such as hydrogenation/dehydrogenation, fuel-cell electrocatalysis, catalytic reforming, ammonia decomposition, and so on.[1,2] In view of the futuristic aspect of the use of hydrogen as a clean fuel and the hurdles in its safe and efficient storage, various advanced research approaches for the development of new materials that can store and deliver hydrogen at acceptable rates have been discovered.[3−5] Unfortunately, even after several decades of exploration, no single material investigated to date meets all of the necessary transportation requirements, such as volumetric and gravimetric hydrogen capacities, handling pressure and temperature, recycling of byproducts, and so on.[3−5] Recent developments in this direction have suggested hydrous hydrazine, such as hydrazine monohydrate ($H_2NNH_2 \cdot H_2O$), which is a liquid over a wide range of temperature (213−392 K),[6] as a promising material for hydrogen storage.[7,8] This material contains a hydrogen content available for hydrogen generation as high as 8.0 wt %, which could be released by complete decomposition of hydrazine to hydrogen and nitrogen via the reaction $H_2NNH_2 \rightarrow N_2 + 2H_2$ (pathway 1), and possesses the distinct advantages of easy recharging and the availability of the current infrastructure of liquid fuels for recharging. Furthermore, besides hydrogen, the only production is nitrogen, which does not need on-board collection for recycling. Moreover, nitrogen, being the most abundant gas in air, can be transformed to ammonia (by the Haber−Bosch process, homogeneous catalytic processes, or an electrolytic process) and then to hydrazine on a large scale or perhaps transformed directly to hydrazine by means of an electrolytic process similar to that for ammonia synthesis.[9] However, to exert the hydrogen storage properties of hydrazine efficiently, its incomplete and undesired decomposition to ammonia by the reaction $3H_2NNH_2 \rightarrow N_2 + 4NH_3$ (pathway 2) must be avoided. Studies have shown a critical dependency of the decomposition of hydrazine via pathway 1 or 2 on the catalyst used and the reaction conditions.[8,10]

Our continuous research activities aiming toward the development of high-performance catalysts for hydrogen generation from hydrous hydrazine under moderate conditions have shown that bimetallic alloy combinations based on nickel and a noble metal (Rh, Pt, or Ir) can lead to complete decomposition of hydrous hydrazine to generate hydrogen selectively.[8] However, despite the high catalytic performance of the bimetallic nanoparticle catalysts (nanocatalysts) investigated to date and our efforts to reduce their noble metal content, the development of a completely noble-metal-free catalyst remains challenging but is crucial for promoting the potential application of hydrous hydrazine as a hydrogen storage material. Herein we report high-performance noble-metal-free bimetallic Ni−Fe nanoparticle catalysts for complete and selective decomposition of hydrous hydrazine to hydrogen under moderate conditions.

Bimetallic Ni−Fe nanocatalysts were prepared using a surfactant-aided coreduction process (Scheme 1). To an aqueous solution of nickel(II) chloride and ferrous(II) sulfate was added an aqueous solution of sodium borohydride in the presence of hexadecyltrimethylammonium bromide (CTAB). $Ni_3Fe$, NiFe, and $NiFe_3$ represent the Ni−Fe nanocatalysts prepared with varying compositions of Ni and Fe, with Ni/Fe molar ratios of 3:1, 1:1 and 1:3, respectively. X-ray photoelectron spectroscopy (XPS) spectra (Figures S1−S3)[11] of the Ni−Fe nanocatalysts exhibit the coexistence of metallic Ni and Fe.[12] In the XPS spectrum of the NiFe nanocatalyst, a thin oxidized layer formed during exposure of the sample to air appears with binding energies for Ni $2p_{3/2}$ at 857.9 eV and for Fe $2p_{3/2}$ at 712.9 eV; this layer can be readily removed by Ar sputtering (Figure S1).[11] Meanwhile, the Ni $2p_{3/2}$ and $2p_{1/2}$ features with binding energies of 852.7 and 870.2 eV, respectively, can be attributed to $Ni^0$, and the Fe $2p_{3/2}$ and $2p_{1/2}$ features with binding energies of 706.7 and 720.1 eV, respectively, can be attributed to $Fe^0$. Furthermore, with periodic Ar sputtering up to 186 min, the relative intensities of the peaks due to $Ni^0$ and $Fe^0$ remain prominent, implying the presence of uniform compositions of Ni and Fe in the NiFe nanocatalyst. Similar XPS patterns have also been observed for the $Ni_3Fe$ and $NiFe_3$ nanocatalysts (Figures S2 and S3).[11] As a result of exposure of the Ni−Fe nanocatalysts, oxides of iron and

**Received:** September 8, 2011
**Published:** November 09, 2011

**Scheme 1. NiFe Nanocatalyst Preparation and Hydrazine Decomposition**

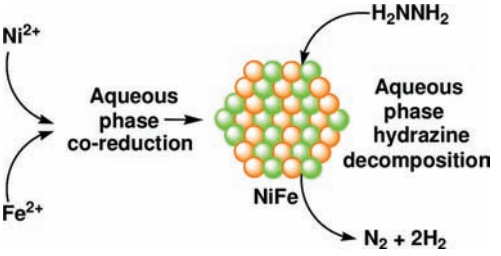


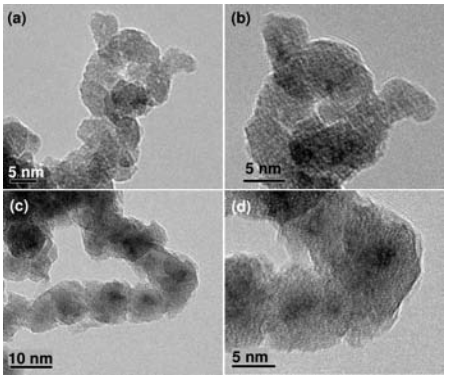


**Figure 1.** (a, c) TEM images and (b, d) corresponding HRTEM images of NiFe nanoparticles.

nickel were formed on the catalyst surface. Since iron is more sensitive to air than nickel, the XPS profiles of $NiFe_3$ nanocatalysts show more oxide layers. Powder X-ray diffraction (PXRD) measurements for the Ni−Fe nanocatalysts illustrate the major diffraction peaks over a $2\theta$ range of 40−50°, which can be indexed to the fcc (111) plane (Figure S4).[11] The diffraction peak for the NiFe nanocatalyst between the fcc diffraction peaks of nickel and iron with a lattice constant of 3.589 Å indicates the homogeneous distribution of Ni and Fe atoms in the NiFe nanocatalyst.

Transmission electron microscopy (TEM) images reveal an average particle size of 10 nm for the NiFe nanoparticles (Figure 1 and Figure S5).[11] The high-resolution TEM (HRTEM) images (Figures 1b,d and 2b) and corresponding selected-area electron diffraction (SAED) pattern (Figure 2b) indicate the crystalline nature of the NiFe nanoparticles. Energy-dispersive X-ray spectroscopy (EDS) point analyses of randomly chosen nanoparticles exhibit the presence of both Ni and Fe (Figure S7).[11]

We further characterized the NiFe nanoparticles by high-angle annular dark-field scanning transmission electron microscopy (HAADF-STEM) and EDS line scanning analyses (Figure 2a). The compositional line profiles of Ni and Fe on the NiFe nanoparticles indicate the uniform alloy composition of NiFe nanoparticles without significant segregation of each component. For the $NiFe_3$ catalyst, TEM and EDS measurements showed that the Ni/Fe ratio is constant at randomly selected points, indicating its uniform alloy composition (Figure S8).[11]

Catalytic decomposition of hydrous hydrazine in the presence of the as-prepared Ni−Fe nanocatalysts was initiated by the introduction of hydrazine monohydrate into the reaction flask, which was vigorously shaken at a constant reaction temperature.

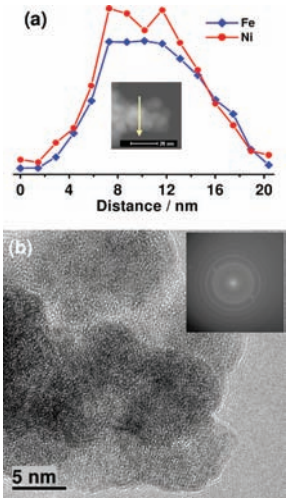


**Figure 2.** (a) Cross-sectional compositional line profiles of Ni and Fe in NiFe nanoparticles recorded along the line shown in the HAADF-STEM image (inset). (b) HRTEM image and the corresponding SAED pattern (inset) for NiFe nanoparticles.

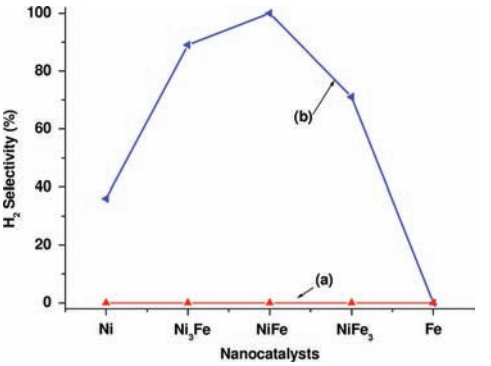


**Figure 3.** Comparison of $H_2$ selectivities in the decomposition of hydrous hydrazine (0.5 M) to hydrogen in the presence of Ni, $Ni_3Fe$, NiFe, $NiFe_3$, and Fe nanocatalysts (catalyst/$H_2NNH_2$ = 1:10) with NaOH (0.5 M) at (a) 298 and (b) 343 K.

The catalytic performance of the nanocatalysts was evaluated on the basis of the volumetrically measured amount of gases released during the reaction. It was recently reported that the catalytic performance of Ni and other related bimetallic nanocatalysts for the decomposition of hydrous hydrazine can be significantly improved with the elevation of the reaction temperature from room temperature to 323 K or higher.[8a] It was also found that the enhancement was not limited to the acceleration of reaction kinetics but was also extensively observed in the selectivity for the decomposition of hydrous hydrazine to hydrogen.

Investigations of the catalytic performance of Ni−Fe nanocatalysts with various Ni/Fe molar ratios for the decomposition of hydrous hydrazine at 343 K suggested a significant dependence of the hydrogen selectivity on the composition of the nanocatalyst. Although the NiFe nanocatalyst exhibited the highest catalytic performance among the examined Ni−Fe nanocatalysts, only 81% hydrogen selectivity was achieved (Figure S9).[11] Surprisingly, it was found that the addition of NaOH significantly enhanced the $H_2$ selectivity (Figure S9).[11] The NiFe nanocatalyst released gases in a stoichiometric amount (3.0 equiv) from


dx.doi.org/10.1021/ja208475y |J. Am. Chem. Soc. 2011, 133, 19638–19641

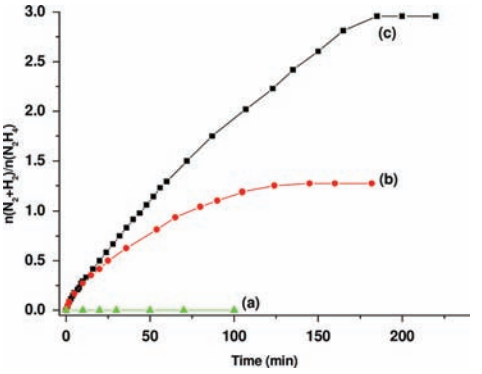


**Figure 4.** Time-course plots for the decomposition of hydrous hydrazine (0.5 M) to hydrogen in the presence of (a) Fe, (b) Ni, and (c) NiFe nanocatalysts (catalyst/$H_2NNH_2$ = 1:10) with NaOH (0.5 M) at 343 K.

the decomposition of hydrous hydrazine in 190 min with NaOH (0.5 M) at 343 K (Figures 3 and 4 and Figure S9), corresponding to complete decomposition of hydrous hydrazine to hydrogen with 100% selectivity via pathway 1. In addition, the NiFe catalyst exhibited high stability (Figure S10).[11] The possible reason for the effects of the alkaline additive might be understood as follows: pathway 2 gives the basic product $NH_3$; the addition of NaOH may make the catalyst surface highly basic, which may be unfavorable for the formation of basic $NH_3$ and therefore for pathway 2. In contrast to the NiFe nanocatalyst, 89% hydrogen selectivity was observed for the $Ni_3Fe$ nanocatalyst, whereas the $NiFe_3$ nanocatalyst exhibited 71% hydrogen selectivity for the decomposition of hydrous hydrazine at 343 K (Figure 3 and Figure S11).[11] Notably, addition of weaker bases (e.g., $NH_3$, $CH_3COONa$) had no effect on the catalytic performance of the NiFe catalysts (Figures S12 and S13).[11] Improvements in the catalytic performance due to addition of NaOH were also observed for $Ni_{45}Pt_{55}$ and $Ni_{50}Ir_{50}$ catalysts; the addition of NaOH (0.5 M) resulted in increases in the $H_2$ selectivity from 61 to 86% for $Ni_{45}Pt_{55}$ and 7 to 95% for $Ni_{50}Ir_{50}$ at 298 K (Figure S14),[11] indicating that the presence of alkaline additives is commonly beneficial in promoting pathway 1.

None of the Ni−Fe nanoparticle catalysts were found to be active for this reaction when examined at 298 K with or without NaOH, indicating the crucial role of temperature in the decomposition reaction (Figure 3). Fe nanoparticles prepared under analogous conditions exhibit no activity for this reaction at 298 K or at elevated temperatures. Ni nanoparticles, which are also inactive at room temperature for the decomposition of hydrous hydrazine, can show an enhancement in the activity with an increase in the reaction temperature.[7,8] An investigation of the role of temperature on the NiFe nanocatalyst showed enhanced activity and $H_2$ selectivity for decomposition of hydrazine to hydrogen at elevated temperatures. Although the NiFe catalyst was inactive at 298 K, the activity was enhanced along with the enhancement in $H_2$ selectivity to 80% at 323 K and 100% at 343 K in the presence of NaOH (0.5 M) (Figure S15).

The enhanced catalytic activities observed for Ni−Fe alloy nanoparticles are of critical importance in view of the fact that their corresponding mononuclear counterparts are either inactive (Fe nanoparticles) or less active (Ni nanoparticles) (Figure 4). Investigations of the catalytic activities under analogous conditions for other bimetallic nanoparticle catalysts prepared using different non-noble metal combinations revealed that the decomposition of hydrous hydrazine is critically influenced by the components of the bimetallic nanocatalyst (Figure S16).[11] In contrast to the significant enhancement of the catalytic activity of the bimetallic NiFe nanoparticle catalyst, the replacement of Fe with Co in NiCo nanoparticle catalysts results in only ~18% hydrogen selectivity, whereas NiCu nanoparticles exhibit ~15% hydrogen selectivity for the decomposition of hydrous hydrazine under analogous reaction conditions. Other bimetallic nanoparticle catalysts obtained by alloying different non-noble metals (e.g., CoCu) exhibited ~15% hydrogen selectivity, whereas the CoFe and FeCu nanoparticle catalysts were found to be catalytically inactive for this reaction under our reaction conditions.

The above results strongly support the conclusion that the catalyst performance is substantially governed by its structure and composition resulting from the introduction of a second component. Considering the poor catalytic performance of the monometallic counterparts, where Fe is inactive and Ni shows low activity for the catalytic decomposition of hydrous hydrazine, the interaction between Ni and Fe in the NiFe alloy, in addition to the effects of temperature and alkaline additives, results in the significant enhancement of the hydrogen selectivity for hydrazine decomposition. The observations make it reasonable to propose that the alloying of Ni and Fe leads to a modification of the catalyst surface through incorporation of considerable intermetallic electronic interactions, and as a result, the presence of both Ni and Fe on the catalyst surface significantly tunes the interactions between the catalyst surface and the hydrazine bonds as well as the stability of the reaction intermediates on the catalyst surface. Consequently, the coexistence of Ni and Fe on the catalyst surface results in the activation of hydrazine preferentially by pathway 1 over pathway 2 for its complete decomposition to hydrogen and nitrogen.

Taking into consideration the previously reported Ni−Rh, Ni−Pt, and Ni−Ir catalysts,[8] alloying Ni and the second metal, as a common feature, at an atomic level is the key to obtaining improved catalytic performance. It should be noted that the combination of Ni and another noble metal with an appropriate Ni/M ratio (M = Rh, Pt, Ni) can achieve 100% $H_2$ selectivity at room temperature without the help of NaOH. However, while the Ni−Fe catalyst requires a higher temperature (343 K) and the coexistence of NaOH to reach 100% $H_2$ selectivity, the present NiFe catalyst is free of noble metals, which is of high importance from the viewpoint of practical use.

In conclusion, we have presented here the development of a highly efficient and low-cost catalyst of nonprecious nickel and iron nanoparticles in alloy form, which achieves 100% hydrogen selectivity from hydrous hydrazine decomposition in an alkaline solution at 343 K. The present finding demonstrates the importance of combining different non-noble metals to develop active metal nanocatalysts whose distinct surface properties enable them to outperform their parent metals. These low-cost, high-performance catalysts may strongly encourage the effective application of hydrous hydrazine as a promising hydrogen storage material.

## ■ ASSOCIATED CONTENT

**Ⓢ Supporting Information.** Details of Ni−Fe nanocatalyst preparation and characterization by PXRD, scanning electron microscopy, TEM, and XPS and the catalytic hydrazine decomposition experiments. This material is available free of charge via the Internet at http://pubs.acs.org.

## AUTHOR INFORMATION


### Corresponding Author

q.xu@aist.go.jp

### Present Addresses

[†]Institute of Inorganic Chemistry, Karlsruhe Institute of Technology (KIT), Geb. 30.45, Engesserstr. 15, D-76131 Karlsruhe, Germany.

### Author Contributions

[‡]These authors contributed equally.


## ACKNOWLEDGMENT

The authors thank the reviewers for valuable suggestions and AIST and JSPS for financial support. S.K.S. thanks JSPS for a postdoctoral fellowship.

## REFERENCES


(1) (a) Jiang, H.-L.; Xu, Q. *J. Mater. Chem.* **2011**, *21*, 13705. (b) Hansgen, D. A.; Vlachos, D. G.; Chen, J. G. G. *Nat. Chem.* **2010**, *2* 484. (c) Ji, X.; Lee, K. T.; Holden, R.; Zhang, L.; Zhang, J.; Botton, G. A.; Couillard, M.; Nazar, L. F. *Nat. Chem.* **2010**, *2*, 286. (d) Kobayashi, H.; Yamauchi, M.; Kitagawa, H.; Kubota, Y.; Kato, K.; Takata, M. *J. Am. Chem. Soc.* **2010**, *132*, 5576. (e) Ferrando, R.; Jellinek, J.; Johnston, R. L. *Chem. Rev.* **2008**, *108*, 845.

(2) (a) Studt, F.; Abild-Pedersen, F.; Bligaard, T.; Sørensen, R. Z.; Christensen, C. H.; Nørskov, J. K. *Science* **2008**, *320*, 1320. (b) Tee, Y.-H.; Grulke, E.; Bhattacharyya, D. *Ind. Eng. Chem. Res.* **2005**, *44*, 7062. (c) Schrick, B.; Blough, J. L.; Jones, A. D.; Mallouk, T. E. *Chem. Mater.* **2002**, *14*, 5140.

(3) (a) Farha, O. K.; Yazaydin, A. Ö.; Eryazici, I.; Malliakas, C. D.; Hauser, B. G.; Kanatzidis, M. G.; Nguyen, S. T.; Snurr, R. Q.; Hupp, J. T. *Nat. Chem.* **2010**, *2*, 944. (b) Chen, B. L.; Xiang, S. C.; Qian, G. D. *Acc. Chem. Res.* **2010**, *43*, 1115. (c) Graetz, J. *Chem. Soc. Rev.* **2009**, *38*, 73. (d) Loges, B.; Boddien, A.; Junge, H.; Beller, M. *Angew. Chem., Int. Ed.* **2008**, *47*, 3962. (e) Xiong, Z.; Yong, C. K.; Wu, G.; Chen, P.; Shaw, W.; Karkamkar, A.; Autrey, T.; Jones, M. O.; Johnson, S. R.; Edwards, P. P.; David, W. I. F. *Nat. Mater.* **2008**, *7*, 138. (f) Stephens, F. H.; Pons, V.; Baker, R. T. *Dalton Trans.* **2007**, 2613.

(4) (a) Luedtke, A. T.; Autrey, T. *Inorg. Chem.* **2010**, *49*, 3905. (b) Hamilton, C. W.; Baker, R. T.; Staubitz, A.; Manners, I. *Chem. Soc. Rev.* **2009**, *38*, 279. (c) Keaton, R. J.; Blacquiere, J. M.; Baker, R. T. *J. Am. Chem. Soc.* **2007**, *129*, 1844. (d) Gutowska, A.; Li, L.; Shin, Y.; Wang, C. M.; Li, X. S.; Linehan, J. C.; Smith, R. S.; Kay, B. D.; Schmid, B.; Shaw, W.; Gutowski, M.; Autrey, T. *Angew. Chem., Int. Ed.* **2005**, *44*, 3578. (e) Chen, Y. S.; Fulton, J. L.; Linehan, J. C.; Autrey, T. *J. Am. Chem. Soc.* **2005**, *127*, 3254.

(5) (a) Jiang, H.-L.; Singh, S. K.; Yan, J.-M.; Zhang, X.-B.; Xu, Q. *ChemSusChem* **2010**, *3*, 541. (b) Yan, J.-M.; Zhang, X.-B.; Akita, T.; Haruta, M.; Xu, Q. *J. Am. Chem. Soc.* **2010**, *132*, 5326. (c) Yan, J.-M.; Zhang, X.-B.; Han, S.; Shiyoyama, H.; Xu, Q. *Angew. Chem., Int. Ed.* **2008**, *47*, 2287. (d) Chandra, M.; Xu, Q. *J. Power Sources* **2006**, *156*, 190.

(6) Schmidt, E. W. In *Hydrazine and Its Derivatives: Preparation, Properties, Applications*, 2nd ed.; Wiley: New York, 1984.

(7) Singh, S. K.; Zhang, X.-B.; Xu, Q. *J. Am. Chem. Soc.* **2009**, *131*, 9894.

(8) (a) Singh, S. K.; Lu, Z.-H.; Xu, Q. *Eur. J. Inorg. Chem.* **2011**, 2232. (b) Singh, S. K.; Xu, Q. *Chem. Commun.* **2010**, *46*, 6545–6547. (c) Singh, S. K.; Xu, Q. *Inorg. Chem.* **2010**, *49*, 6148. (d) Singh, S. K.; Xu, Q. *J. Am. Chem. Soc.* **2009**, *131*, 18032.

(9) (a) Hazari, N. *Chem. Soc. Rev.* **2010**, *39*, 4044. (b) Chin, J. M.; Schrock, R. R.; Müller, P. *Inorg. Chem.* **2010**, *49*, 7904.(c) Smil, V. In *Enriching the Earth: Fritz Haber, Carl Bosch and the Transformation of World Food Production*; MIT Press: Cambridge, MA, 2004. (d) Murakami, T.; Nishikiori, T.; Nohira, T.; Ito, Y. *J. Am. Chem. Soc.* **2003**, *125*, 334. (e) Sridhar, S.; Srinivasan, T.; Virendra, U.; Khan, A. A. *Chem. Eng. J.* **2003**, *94*, 51. (f) Hayashi, H. *Res. Chem. Intermed.* **1998**, *24*, 183. (g) Hayashi, H. *Catal. Rev.* **1990**, *32*, 229.

(10) (a) Cho, S. J.; Lee, J.; Lee, Y. S.; Kim, D. P. *Catal. Lett.* **2006**, *109*, 181. (b) Zheng, M.; Cheng, R.; Chen, X.; Li, N.; Li, L.; Wang, X.; Zhang, T. *Int. J. Hydrogen Energy* **2005**, *30*, 1081. (c) Chen, X.; Zhang, T.; Zheng, M.; Wu, Z.; Wu, W.; Li, C. *J. Catal.* **2004**, *224*, 473. (d) Santos, J. B. O.; Valença, G. P.; Rodrigues, J. A. J. *J. Catal.* **2002**, *210*, 1. (e) de Mederios, J. E.; Valença, G. P. *Braz. J. Chem. Eng.* **1998**, *15*, 86–96.(f) Armstrong, W. E.; Ryland, L. B.; Voge, H. H. U.S. Patent 4,124,538, 1978.

(11) See the Supporting Information.

(12) Moulder, J. F.; Chastain, J.; King, R. C. In *Handbook of X-ray Photoelectron Spectroscopy: A Reference Book of Standard Spectra for Identification and Interpretation of XPS Data*; Physical Electronics: Eden Prairie, MN, 1995.